Materials Transactions, Vol. 42, No. 11 (2001) pp. 2316 to 2321
Special Issue on Advances in Computational Materials Science and Engineering II

Modeling of As-Cast Microstructure of Al Alloy with a Modified Cellular Automaton Method

Q. Y. Xu and B. C. Liu

Department of Mechanical Engineering, Tsinghua University, Beijing 100084, P.R. China

Microstructure modeling of aluminum alloy casting has been carried out by using a modified cellular automaton (CA) method coupled with macro heat transfer calculation. Continuous nucleation model is applied to describe heterogeneous nucleation in liquid metal. Dendrite tip growth kinetics and preferential ⟨100⟩ crystallographic orientation are taken into account. Therefore, the stochastic nature of nucleation process as well as the deterministic of dendrite growth is considered to simulate the crystal growth. The actual dendritic shape is substituted for the square envelope in the ordinary cellular automaton model. In addition, the coordinate transformation method is employed to describe the grain growth and to maintain it onto the original orientation of nucleus. Simulation results show that grain size is different at various positions of a step-shaped sample casting. The grain size is smaller when cooling rate is faster and vice versa, which is in good agreement with the experimental results and the solidification mechanism as well.

(Received April 4, 2001; Accepted June 11, 2001)

Keywords: *microstructure modeling, modified cellular automaton model, nucleation and growth, solidification*

1. Introduction

The control of grain structure is of significant importance in solidification process, since the grain structure has a direct influence on the mechanical properties of product. Great efforts have been made to predict the maps of grain structures. Many methods have been proposed to model the grain structure. Among them, deterministic models[1)] have coupled the micro-model with macroscopic heat flow equation. As a result, the average size of equiaxed grains and the longitudinal extension of columnar grains can be calculated. However, since these models neglect the aspect related to crystallographic effect, they cannot account for the competition of grains in the columnar region, nor for the transition from the outer equiaxed zone to the columnar zone, which occurs near the mold wall surface of casting. The phase-field method presented by Karma and Rappel[2)] is limited to relatively high supercoolings and to relatively small equiaxed grain without a full side-branch structure. The extension to fully dendritic grains growth at the low supercoolings for casting process would require an increase in computational power by at least three orders of magnitude in both speed and memory. Spittle and Brown[3)] were the first to adopt the Monte Carlo method for the prediction of grain structures of casting. Rappaz and Gandin[4,5)] introduced a physically-based cellular automaton (CA) approach which integrated a growth kinetics model and the preferential growth direction of dendrites (*i.e.* ⟨100⟩ crystallographic orientations for cubic materials). However, the growth direction of grains was mis-oriented from the original orientation in CA model. In addition, the dendrite growth velocities were calculated based on some local mean undercooling, and the temperature (or concentration) field between the grains was not solved. Consequently, it is difficult by using cellular automaton model to provide a detail study of the local growth interactions and to describe some features in detail such as side branching.

Therefore, modeling of equiaxed dendrite solidification in the present study is facilitated by a modified cellular automaton model that combines the CA model and the actual envelope of dendrite. A new approach, the coordinate transformation method, is proposed to overcome the mis-orientation of grain growth.

2. Mathematical Formula

In order to predict the grain structure accurately, the cellular automaton method is combined with the deterministic modeling, which is based on the physical mechanism of nucleation and the kinetic theory of grain growth. The distribution of nucleus position is treated in the way as the deterministic method. During the calculation, the cells can solidify according to the mechanisms of heterogeneous nucleation and grain growth when the temperature becomes lower than the liquidus. The grain density is calculated in a deterministic way by using the distribution of nucleation sites which become active as the undercooling increases. However, the location and crystallographic orientation of new grains nucleated in the liquid are chosen randomly among the liquid cells and a certain number of classes of possible orientations, respectively. The growth kinetics of the dendrite tips and the ⟨100⟩ preferential growth direction are implemented in the model in the way described in Sections 2 and 3 that the original crystallographic orientation of the nuclei is kept during the entire growth process.

2.1 Mesh generation and the calculation of temperature of micro-cells

The coarse macro cells are used to calculate the temperature field in the solidifying region. The macro cell is divided into many micro-cells for the calculation of nucleation and grains growth as shown schematically in Fig. 1. The size of CA grid is in the scale of μm, which is compatible with that of dendrite arm spacing.

The temperature of CA cells should be calculated first in microstructure simulation. Due to the small size of the micro-cell (in the order of magnitude of μm), it will

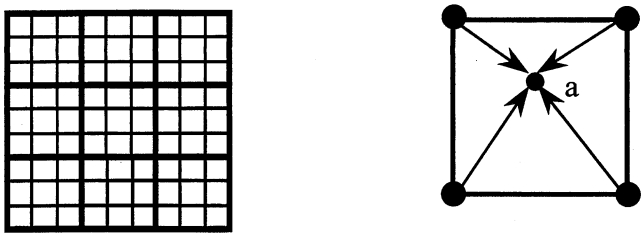

Fig. 1 The relation between macro and micro cells (2-dimension).

take much more time if the temperature filed of micro-cells is calculated by numerical heat transfer method. Therefore, micro-cells temperature is obtained by 2D interpolation method. Obviously the temperature of a CA cell is influenced by its nearest neighboring macro-cells, and hence the interpolation formula can be constructed according to the thermal contribution of macro-cells, *i.e.* the temperature of the CA cell is in reverse ratio to the distance between the neighboring macro-cell and point "a":

$$T_{\mathrm{a}} = \sum_{i=1}^{4} l_i^{-1} T_i \Big/ \sum_{i=1}^{4} l_i^{-1} \tag{1}$$

Where T_{a} is the temperature of the CA cell "a", T_i is the temperature of the neighboring macro-cell, and l_i is the distance from "a" to the macro-cell.

2.2 Nucleation model

There are two mathematical ways that can be used for the calculation of the heterogeneous nucleation, *i.e.* instantaneous nucleation and continuous nucleation. Considering the physical fundamental of nucleation process, the continuous nucleation model is used to describe the nuclei formed in the liquid during solidification. The increase of grain density, $\mathrm{d}n$, which corresponds to an undercooling increase, $\mathrm{d}(\Delta T)$, can be described by a continuous nucleation distribution, $\mathrm{d}n/\mathrm{d}(\Delta T)$. A Gaussian distribution is chosen in the present study. The density of grains at a given undercooling is thus given by the integral of this distribution,

$$n(\Delta T) = \int_0^{\Delta T} [1 - f_{\mathrm{s}}(\Delta T')] \frac{\mathrm{d}n}{\mathrm{d}(\Delta T')} \mathrm{d}(\Delta T') \tag{2}$$

and

$$\frac{\mathrm{d}n}{\mathrm{d}(\Delta T')} = \frac{n_{\max}}{\sqrt{2\pi}\Delta T_\sigma} \exp\left[-\frac{1}{2}\left(\frac{\Delta T' - \Delta T_{\mathrm{N}}}{\Delta T_\sigma}\right)^2\right] \tag{3}$$

where ΔT_{N} is the mean nucleation undercooling, ΔT_σ is the standard deviation, $n_{\max}$ is the total density of grains, and f_{s} is the volume fraction of solid phase.

During one time-step, δt, the temperature of the micro cell decreases by an amount, δT, and thus the undercooling increases by an amount $\delta(\Delta T)$ (> 0). Accordingly, the density of new grains which are nucleated in the undercooling melt is given by:

$$\begin{aligned} \delta n &= n[\Delta T + \delta(\Delta T)] - n(\Delta T) \\ &= \int_{\Delta T}^{\Delta T + \delta(\Delta T)} \frac{\mathrm{d}n}{\mathrm{d}(\Delta T')} \mathrm{d}(\Delta T') \end{aligned} \tag{4}$$

The number of new grains in this time-step is given by the multiplication of the grain density increase δn with the total volume of the melt. The location of these new grains is randomly chosen among the CA cells which are still liquid by defining the corresponding probability p,

$$p = \delta N / N_{\mathrm{CA}} = \delta n V_{\mathrm{CA}} \tag{5}$$

where N_{CA} is the total number of cells in volume V, and V_{CA} is the volume of one CA cell. During one δt, each CA cell is assigned a random number r ($0 \le r \le 1$). If a cell is still liquid, the transformation from liquid to solid will occur when

$$r \le p \tag{6}$$

2.3 Growth model

2.3.1 Undercooling in front of dendrite tip

The total undercooling in front of dendrite tip, ΔT, is generally the sum of the four contributions:[6]

$$\Delta T = \Delta T_c + \Delta T_t + \Delta T_k + \Delta T_r \tag{7}$$

where ΔT_c, ΔT_t, ΔT_k and ΔT_r are the undercooling contributions associated with solute diffusion, thermal diffusion, attachment kinetics and solid-liquid surface curvature, respectively. For most of metallic alloys, ΔT_t and ΔT_k have little effect on the total undercooling, while the constitutional and curvature undercooling are predominant under normal casting condition. Therefore,

$$\Delta T = T_{\mathrm{L}}^{\mathrm{EQ}} + (c_l^* - c_0)m - \Gamma K - T^* \tag{8}$$

where $T_{\mathrm{L}}^{\mathrm{EQ}}$ is the equilibrium liquidus temperature of the alloy, m is the liquidus slope of the phase diagram, K is the mean curvature of the solid/liquid interface, Γ is the Gibbs-Thomson coefficient, c_l^* is the solute concentration at the solid/liquid interface, c_0 is the initial concentration of the alloy in the liquid, and T^* is the temperature at the interface. In order to obtain undercooling at the interface, the concentration field near the dendrite tips must be resolved either by numerical calculation or simply by Scheil equation:

$$c_l^* = c_0(1 - f_{\mathrm{s}})^{k-1} \tag{9}$$

where k is the partition coefficient.

Another term in the eq. (7) is the curvature undercooling, which can be calculated by the determination of the curvature K at the interface:[7]

$$K = \left\{1 - 2\left[f_{\mathrm{s}} + \sum_{i=1}^{N} f_{\mathrm{s}}(i)\right] \Big/ (N+1)\right\} / l \tag{10}$$

where l is the mesh size of micro-cells, and N is the number of neighboring cells.

2.3.2 Growth kinetics of dendrite tip

The growth velocity of dendrite tip can be calculated by KGT model.[8] The dendrite tip radius R, and the growth ve-

locity v are determined by the following two relationships:

$$R = 2\pi[\Gamma/(mG_c\xi_c - G)]^{1/2} \quad (11)$$

$$\Omega = (c_l - c_0)/[c_l(1-k)] = Iv(Pe) \quad (12)$$

where Ω is the supersaturation, c_l is the concentration in the liquid at the tip, k is the partition coefficient, G_c is the solute concentration gradient in front of dendrite tip in the liquid, and G is the temperature gradient.

Pe is the solute Péclet number, $Pe = Rv/(2D)$. $Iv(Pe)$ is Ivantsov function of Péclet number, ξ_c is also the function of Péclet number. v is the growth velocity of dendrite tip, and D is the solute diffusion coefficient in the liquid.

In the dendritic region, G can be neglected and ξ_c is close to 1 at low growth velocity. The undercooling ΔT is the function of the supersaturation Ω as follows:

$$\Delta T = mc_0[1 - 1/(1 - \Omega(1-k))] \quad (13)$$

Combining the above eqs. (11)–(13), the growth velocity of dendrite tip can be derived as follows:

$$(1-\Omega)^2\pi^2\Gamma v^2 + \Omega^2 Dmc_l(1-k)v + \Omega^2 GD^2 = 0 \quad (14)$$

2.3.3 Growth direction

The preferential growth direction of cubic metal is ⟨100⟩ orientation. For 2D cellular automaton method, only two orientations, ⟨10⟩ and ⟨01⟩, are considered in the calculation. Assumed that the grains nucleated in liquid have random crystallographic orientation, the probability of the new grain orientation located in $[\theta, \theta + d\theta]$ is:

$$dp(\theta) = 2d\theta/\pi \quad (15)$$

3. Modification of CA Model

3.1 CA model by Gandin and Rappaz

The cellular automaton model by Gandin and Rappaz can describe the dendritic growth with a cubic crystal structure.[4,9,10] For 2D calculation, a uniform network of square cells is used in which each cell represents a small discrete area and is characterized by a state index (liquid or solid) and a temperature value. In case of uniform thermal field, the envelope of a dendritic grain with cubic structure can be considered as an almost square shape in 2D, which represents the anisotropic growth along the preferential ⟨100⟩ orientation. In CA calculation, a growing square is assumed to describe the growth of a grain.

The schematic representation of cellular automaton model[4] is shown in Fig. 2. 'A' is a nucleation site in mesh grids which is nucleated at a certain time t_N. The direction of the maximum growth velocity deviates θ from x axis ($-45° < \theta < 45°$). At time t, the radius of grain $L(t)$, *i.e.* the semi-diagonal of the shadowed square in Fig. 2, is the integral along the whole growing time:

$$L(t) = \int_v v[\Delta T(t')]dt' \quad (16)$$

$v[\Delta T]$ can be calculated by the previous KGT model. At the time t_B, the grain nucleated at site A grows and touches the four neighboring cells B1, B2, B3 and B4, when $L(t_B)$ is equal to $l_\theta = l(\cos\theta + |\sin\theta|)$ in which l is the grid spacing of CA cells. Then B1 ~ B4 are considered to become solid and assigned a crystallographic index same as site A. The 4 sites of B continue to grow and capture their neighboring sites at the next time t_C, *etc.* However, the growth direction of the grain deviates from its original orientation, and therefore it is necessary to modify the cellular automaton model in order to correct the growth direction of dendrite grains. In addition, the growth shape of grains is considered as square shape in the model, which is also different from the real physical phenomenon.

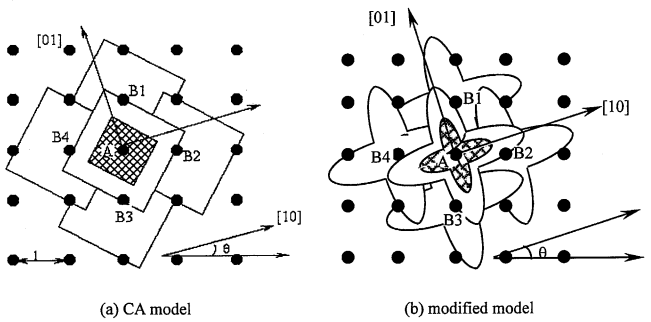

(a) CA model (b) modified model

Fig. 2 Schematic diagram of Cellular Automaton model (shadow area represents a growing grain).

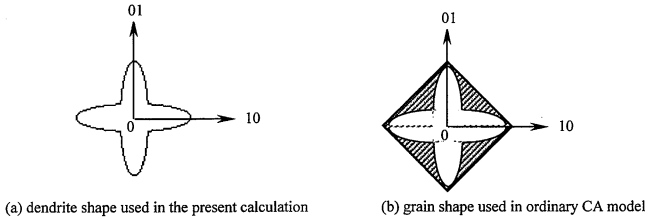

(a) dendrite shape used in the present calculation (b) grain shape used in ordinary CA model

Fig. 3 Actual equiaxed dendrite shape in 2D.

3.2 New modified CA model

3.2.1 Grain shape assumed to be dendritic instead square shape

In fact, the envelope of the grains growing freely in the liquid is dendritic, and it can be treated as shown in Fig. 3(a). Compared to the dendritic shape, the square shape would capture much more cells than it should, *i.e.*, the cells locate in the shadow as shown in Fig. 3(b).

There are two ways to describe the envelope of the grain, that is mathematical and experimental methods. In the paper a shape function $L(\theta)$ is introduced:

$$L(\theta) = L_0[1 + (A-1)\cos 4\theta] \quad (17a)$$

or,

$$L(\theta) = L_1[B + (1-B)\cos 4\theta] \quad (17b)$$

where, $A = L_1/L_0$, $B = L_0/L_1$, L_0 and L_1 are defined as in Fig. 4, in which a unit cell is depicted.

The factor A or B determine the anisotropy of the shape function. The maximum value of A is 2, and a circular shape with A of 1 can describe the cellular growth.

The function is chosen according to the description of the surface free energy of bcc crystals. Under the condition of high thermal gradient and low cooling rate, the tertiary arms could be neglected, and so the shape function is a good geometric approach.

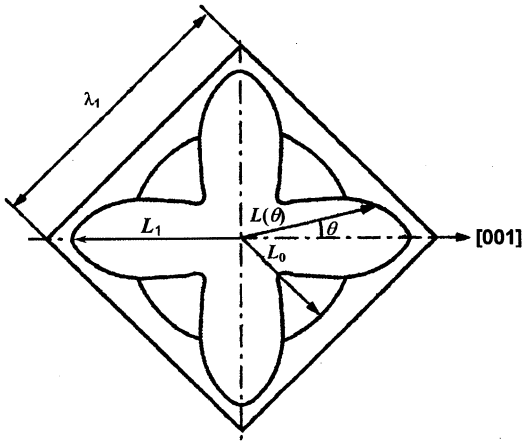

Fig. 4 Shape function $L(\theta)$ in a unit cell of length λ_1.

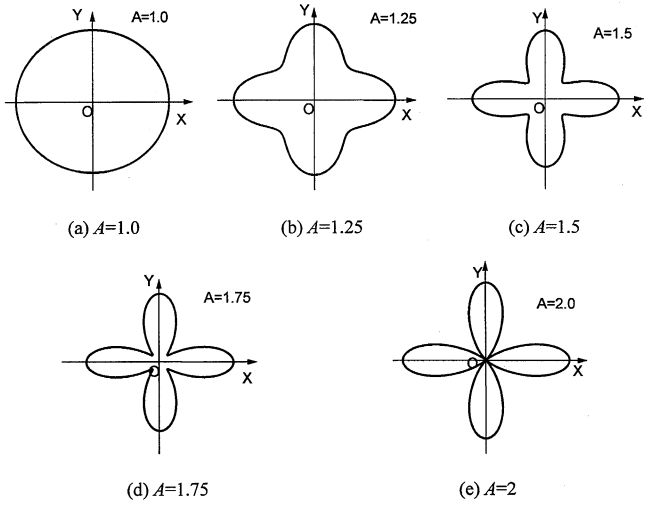

(a) A=1.0 (b) A=1.25 (c) A=1.5

(d) A=1.75 (e) A=2

Fig. 5 Variation of dendrite shape with the factor A.

The side length of the unit cell is correlated to the dendritic primary arm spacing λ_1, and can be estimated from the thermal gradient G and the solidification velocity v with the theory of Hunt:[11]

$$\lambda_1 = KG^{-1/2}v^{-1/4} \tag{18}$$

K can be measured by experiments and L_1 can be calculated with the numerical method during the growth. Therefore, the shape of the dendrite will be determined by the factor A or B, which depends on the growth conditions, the diffusion coefficient and surface energy. The influence of the factor A/B on the dendrite shape is shown in Fig. 5. When $A = 1.5$–1.75 the shape is very close to the real dendritic shape.

3.2.2 Coordinate transformation method to overcome the mis-orientation of grain from original direction during the growth

In the previous model,[4,9,10] the growth direction of grains is mis-oriented by an angle δ from the original orientation during further growth. It was found that the ordinary CA algorithm can works well if the ⟨100⟩ orientation coincides with the grid orientation (0°, 90°, 180°, 270°). Since there is no mis-orientation of grain growth when ⟨100⟩ direction coincides with x axis, the coordinate transformation method is employed to make the growth direction of grains along the coordinate axes as shown in Fig. 6.

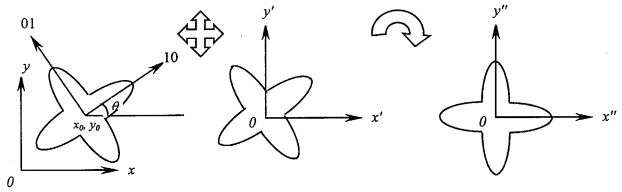

(a) original position and orientation (b) parallel translation (c) rotation

Fig. 6 Coordinate transformation of an equiaxed grain growing in the liquid.

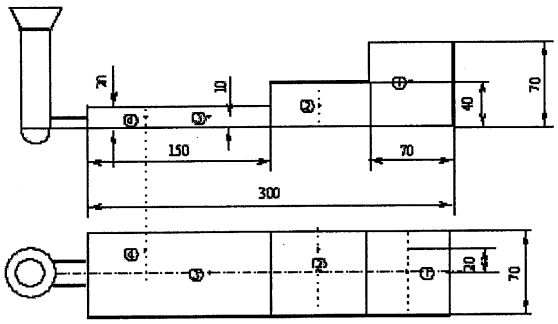

Fig. 7 Sample casting shape and the positions for modeling.

It is assumed that a grain nucleates at (x_0, y_0) in xoy coordinate system, and its orientation is characterized by an angle θ. In order to keep the coincidence of the ⟨100⟩ growth orientation of the grain with the coordinate axis, several steps must be taken as depicted in Fig. 6. Firstly the origin of xoy system moves to the grain's nucleus center to form the $x'oy'$ coordinate system by parallel translation. Then the $x'oy'$ system rotates an angle θ in counterclockwise direction to form the $x''oy''$ coordinate system. In $x''oy''$ system, the nucleated grain grows in the direction of coordinate axis ox'' or oy''. After a grain grows completely it is transferred to the original xoy coordinate system.

4. Experiments

In order to validate the modeling results, some experiments were carried out and step-shaped samples were cast with Al–Si alloy in sand mold. The sample shape and size are schematically shown in Fig. 7. The experimental condition is shown in Table 1. The chemical composition of the cast alloys is listed in Table 2.

Al–Si alloy was melted in a pit type resistance furnace under covered flux (45% NaCl–45% KCl–10% NaF), and the melt was held at 760°C. After degassing with hexachloroethane, it was directly cast into a green sand mold. In order to record the thermal history of the alloy during cooling, four 0.3 mm diameter type K thermocouples with alumina sheath 1.5 mm diameter were located at the four positions of the sand mold cavity as shown in Fig. 7. The tip of the thermocouples was in direct contact with the alloys and the thermocouple outputs are recorded on a personal computer with data recording and processing facilities. After solidification, the specimens were sectioned for metallographic examinations. After electropolishing in an electrolytic bath comprising of

Table 1 Experimental and measurement conditions.

Casting material	Al–Si alloy
Casting method	sand mold
Pouring temperature	750°C
Acquiring speed	150 μs/point
Acquiring frequency	200 ms (solidification process after mold filling)
Total acquiring time	900 s (solidification process after mold filling)
Acquiring accuracy	±5°C
Total sample points of each cooling curve	> 4, 500 points

Table 2 Chemical composition of the testing alloy (in wt.%)

% Si	% Cu	% Mg	% Mn	%Al
7.5	2.0	0.5	0.5	Balance

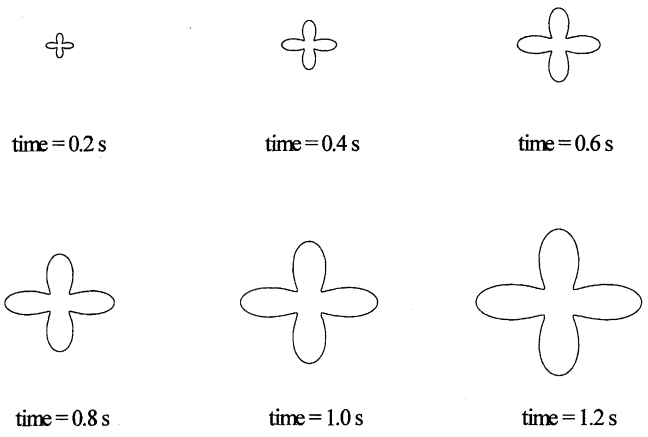

Fig. 8 Equiaxed dendritic growth of a single grain at various solidification time.

80% methanol and 20% HNO_3, the polished surface of samples was then etched with Keller's reagent (2.5% HNO_3, 1.5% HCl, 1% HF and 95% H_2O).

5. Results and Discussion

5.1 A single equiaxed grain growing in the melt

A single equiaxed grain's growth in the undercooling melt was simulated. In calculation, the shape factor $A = 1.6$ and the undercooling $\Delta T = 10.0$ K. The whole calculation domain was divided into 200 × 200 CA cells with the mesh size $\Delta x = \Delta y = 5\,\mu$m. The equiaxed grain growth morphology at different solidification time is shown in Fig. 8. It is indicated that the above concept can be used to depict the dendrite evolution morphology in the solidification process including the coarsening of the primary trunk and the branching of the secondary arm. The simulated grain feature of the free dendritic growth is in good agreement with the previous experiments reported by Glicksman.[12)]

5.2 Simulation of grain structure in a step-shaped sample casting

Microstructure calculation scheme and post-processing module were developed based on the above algorithm. The grain structure prediction of Al–Si alloy was carried out and

Table 3 Thermophysical parameters of Al–Si alloy.

Thermal conductivity, λ/W/(m·°C)	125
Specific heat, ρc_p/[J/(m^3·°C)]	2.96×10^6
Latent heat, ΔH_f/(J/m^3)	9.5×10^8
Melting point, T_m/(°C)	615
Eutectic temperature, T_{eut}/(°C)	577
Partition coefficient, K	0.117
Slope of liquidus, m/(°C/%)	−6

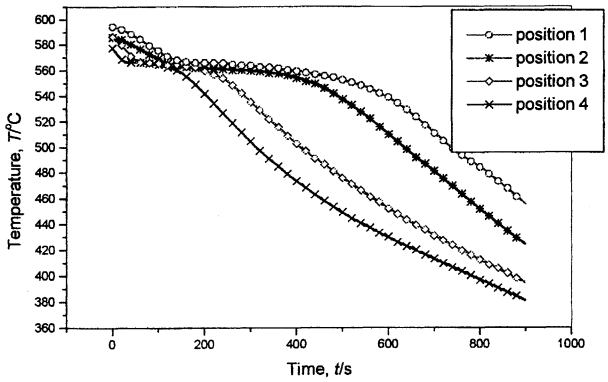

Fig. 9 Cooling curves at different positions of sample casting.

the thermophysical parameters used in the calculation are shown in Table 3.

The microstructure of the step-shaped sample (shown in Fig. 7) was calculated with the modified Cellular Automaton method. The size of macro-cell for the calculation of heat transfer is 10 mm × 10 mm × 10 mm, and is further divided into 500 × 500 CA cells. The microstructures at positions (1), (2), (3) and (4) of casting as shown in Fig. 7 were calculated respectively.

The measured cooling curves during solidification at the four positions of the sample casting are shown in Fig. 9, while the corresponding microphotographs are shown in Fig. 10. The dendrites are clearly revealed in these microphotographs by electrolytic etching. From the orientation of these dendrites, grain contours can be estimated by visual inspection.

The calculated grain structures of four different positions are shown in Fig. 11. The thinner the thickness, the larger the cooling rate, and the smaller the grains. Both experimental results and simulation calculation indicated that the grain size becomes smaller and smaller from positions (1) to (4) due to the increase of cooling rate.

6. Conclusions

(1) Several important issues were discussed with the CA model, such as the nucleation and growth of grains, the corresponding numerical algorithms and the temperature interpolation of micro CA cells.

(2) Combining the advantages of deterministic modeling, a modified cellular automaton model was studied and established in several aspects, such as the actual dendritic envelope and new growth algorithm based on the coordinate transformation method in order to maintain the crystal growth orientation.

(3) The modified cellular automaton model was then used

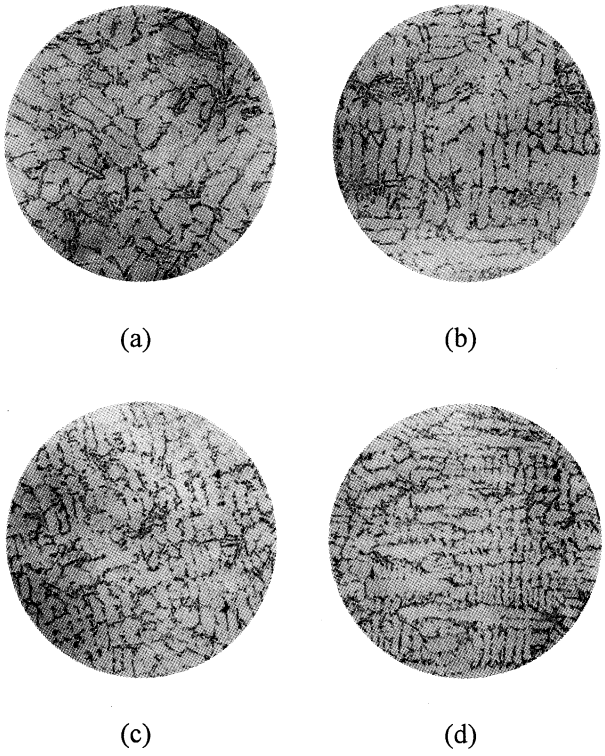

Fig. 10 Optical microphotographs of the step-shaped sample casting at different positions.

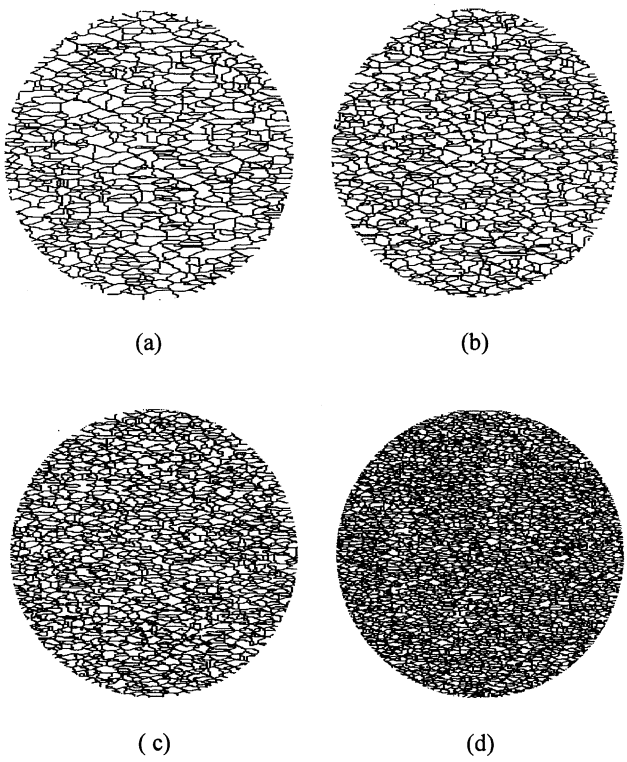

Fig. 11 Calculated grain contour of Al–Si alloy at different positions.

to calculate the microstructure of Al–Si alloy coupling with macro heat transfer. The grain structure was calculated at four different positions of a step-shaped sample casting especially designed for verification. The predicted grain structure is in good agreement with the actual optical microphotographs.

Acknowledgements

The research was sponsored by the Significant Project of National Natural Science Foundation of China (No. 59990470–3), and the National Significant Fundamental Research Project of the Ministry of Science and Technology of China (No. G2000067208–3) and the Key Fundamental Research Project of Tsinghua University.

REFERENCES

1) D. M. Stefanescu and C. S. Kanetkar: AFS Trans. **95** (1987) 139–144.
2) A. Karmar and W. Rappel: Phys. Rev. Lett. **77** (1996) 4050–4053.
3) S. G. R. Brown and J. A. Spittle: Mater. Sci. Technol. **5** (1989) 362–368.
4) M. Rappaz and Ch.-A. Gandin: Acta Metall. Mater. **41** (1993) 345–360.
5) Ph. Thévoz, J.-L. Desbiolles and M. Rappaz: Metall. Trans. **20A** (1989) 311–322.
6) M. C. Flemings: *Solidification Process*, (McGraw-Hill, New York, 1974) pp. 134–176.
7) L. Nastac: *Proceedings of Modeling of Casting and Solidification Processes IV*, 1999. ed. By C. P. Hong, J. K. Choi and D. H. Kim, pp. 31–42.
8) W. Kurz, B. Giovanola and R. Trivedi: Acta Metall. **34** (1986) 823–830.
9) Ch.-A. Andin, M. Rappaz and R. Tintillier: Metall. Trans. **24A** (1993) 467–479.
10) Ch.-A Gandin and M. Rappaz: Acta Mater. **45** (1997) 2187–2195.
11) J. D. Hunt, D. T. J. Hurle, K. A. Jackson and E. Jakeman: Metall. Trans. **1** (1970) 318–320.
12) M. E. Glicksman, E. Winsa, R. C. Hahn, T. A. Lograsso, S. H. Tirmizi and M. E. Selleck: Metall. Trans. **19A** (1988) 1945–1953.